Annals of Botany **114**: 841–851, 2014
doi:10.1093/aob/mcu009, available online at www.aob.oxfordjournals.org

ANNALS OF BOTANY
Founded 1887

PART OF A SPECIAL ISSUE ON FUNCTIONAL–STRUCTURAL PLANT MODELLING

An integrated method for quantifying root architecture of field-grown maize

Jie Wu and Yan Guo*

Key Laboratory of Arable Land Conservation (North China), Ministry of Agriculture, College of Resources and Environmental Sciences, China Agricultural University, Beijing 100193, China
** For correspondence. E-mail yan.guo@cau.edu.cn*

Received: 16 October 2013 Returned for revision: 20 December 2013 Accepted: 8 January 2014 Published electronically: 15 February 2014

• **Background and Aims** A number of techniques have recently been developed for studying the root system architecture (RSA) of seedlings grown in various media. In contrast, methods for sampling and analysis of the RSA of field-grown plants, particularly for details of the lateral root components, are generally inadequate.
• **Methods** An integrated methodology was developed that includes a custom-made root-core sampling system for extracting intact root systems of individual maize plants, a combination of proprietary software and a novel program used for collecting individual RSA information, and software for visualizing the measured individual nodal root architecture.
• **Key Results** Example experiments show that large root cores can be sampled, and topological and geometrical structure of field-grown maize root systems can be quantified and reconstructed using this method. Second- and higher order laterals are found to contribute substantially to total root number and length. The length of laterals of distinct orders varies significantly. Abundant higher order laterals can arise from a single first-order lateral, and they concentrate in the proximal axile branching zone.
• **Conclusions** The new method allows more meaningful sampling than conventional methods because of its easily opened, wide corer and sampling machinery, and effective analysis of RSA using the software. This provides a novel technique for quantifying RSA of field-grown maize and also provides a unique evaluation of the contribution of lateral roots. The method also offers valuable potential for parameterization of root architectural models.

Key words: Branching order, lateral roots, root system architecture, topological structure, root architectural model, maize, *Zea mays*.

INTRODUCTION

Root system architecture (RSA), the topological arrangement of component root types and their geometrical characteristics, plays a key role in determining plant water and nutrient uptake (Fitter, 1987; Lynch, 1995; Danjon and Reubens, 2008). The RSA varies greatly between species and between individuals of any particular genotype, and has high plasticity responding to soil environmental change (Hodge, 2004; Malamy, 2005; Nibau *et al.*, 2008; Gruber *et al.*, 2013). Lateral roots, especially of cereal crops, comprise the major part of a root system in terms of root length (Dittmer, 1937; Hackett and Rose, 1972; Yamauchi *et al.*, 1987; Varney *et al.*, 1991; Bouma *et al.*, 2001) and root number (Iijima *et al.*, 1991). The growth of lateral roots responds to the heterogeneity of the soil environment (Hodge, 2004, 2006) and is influenced by their developmental instability (Forde, 2009). Research shows that lateral roots are commonly highly variable in branch length, branch density and the inter-lateral root distance of first-order laterals, and this remains true even when grown under controlled conditions (Varney *et al.*, 1991; Pagès and Pellerin, 1994; Nibau *et al.*, 2008; Forde, 2009; Dubrovsky and Forde, 2012). On the other hand, the heritability of RSA traits highlights its significance in crop breeding programmes (de Dorlodot *et al.*, 2007; Lynch and Brown, 2012; Smith and Smet, 2012; Galkovskyi *et al.*, 2012). Recently, root branching has attracted renewed attention, and the importance of measuring RSA traits (including the numbers and lengths of laterals) is emphasized for realizing the power of comparative genetics (de Dorlodot *et al.*, 2007).

The opacity of soil media is a key limitation to accurate and rapid measurement of RSA in the field. Researchers have developed alternative, laboratory-based, technologies for studying the root systems of seedlings grown in non-soil or soil media. Digital cameras, flat-bed scanners and three-dimensional (3-D) laser scanners have been used to measure and extract static and dynamic RSA traits of young plants grown in transparent gel media, non-invasively and with high resolution (Armengaud *et al.*, 2009; Fang *et al.*, 2009; Iyer-Pascuzzi *et al.*, 2010; Clark *et al.*, 2011, 2013). However, the target plants are very young and so their root systems exhibit relatively simple branching patterns. Furthermore, due to the influence of the medium, the results of root trait screens from non-soil media may be significantly different from, or even opposite to, those expressed under soil media (McCully, 1999; Gregory *et al.*, 2009; Clark *et al.*, 2011). The detailed conditions of laboratory or greenhouse experiments, such as pot size, may also influence data comparability (Poorter *et al.*, 2012).

To image and quantify RSA in soil media, a number of non-destructive approaches have been applied, including X-ray micro-computed tomography (CT) (Flavel *et al.*, 2012; Mairhofer *et al.*, 2012; Mooney *et al.*, 2012), neutron tomography (Moradi *et al.*, 2011), magnetic resonance imaging (Pohlmeier *et al.*, 2008; Jahnke *et al.*, 2009; Rascher *et al.*, 2011) and nuclear magnetic resonance (Rogers and Bottomley,

1987; Brown *et al.*, 1991; Menzel *et al.*, 2007). However, their application in the field is obstructed by their limited container size (<3 cm in diameter for using X-ray micro-CT), high cost and the fact that the interference of soil water, organic matter, aggregates and paramagnetic ions cannot be avoided (Flavel *et al.*, 2012).

Field excavation had been used for a long time to extract comparatively complete root systems of individual plants (Weaver *et al.*, 1924; Pavlychenko, 1937; Nelson and Allmaras, 1969; Bohm, 1979; Pagès and Pellerin, 1994; Fiorani and Schurr, 2013). However, it is extremely laborious and time consuming, and heavy machinery is required. The soil around the focal volume can also be significantly disturbed. One of the major disadvantages of this method is the breakage of root connections which often results in a severe loss of information, especially with regard to the topological inter-relations of root laterals of different orders (Pagès and Pellerin, 1994). Although shovelomics has been proposed as a high-throughput method for phenotyping roots in the field (Trachsel *et al.*, 2010), acquiring detailed data on the length and number of laterals of different orders was not its target.

Maize is one of our most important crops. It forms complex root architectures composed of a range of different root types (Hochholdinger *et al.*, 2004), especially for field-grown maize after plant tasselling (Peng *et al.*, 2010). However, due to both the extreme complexity of its root architecture and the lack of appropriate field sampling methods, a thorough understanding of the RSA of field-grown maize is lacking.

In this study, an integrated technique is presented for collecting detailed topological and geometrical information of the root systems (including laterals) of field-grown crops such as maize. It includes: a custom-made root-core sampling system to excavate the major part of the root system of an individual plant, the use of proprietary software for root image analysis to process and extract topological and geometrical information of axile and lateral roots, a novel program for organizing the data, and software for visualizing individual nodal roots based on extracted data. The RSA of a maize plant 19 days after silking was quantified.

MATERIALS AND METHODS

Field experiment

The field experiment was conducted in 2011 at the Shangzhuang Experimental Station (40°08′N, 116°10′E) of China Agricul-tural University. The soil type is an aquic cambisol with a sandy clay loam texture (FAO). The maize hybrid ZD958 (*Zea mays* L.) was sown on May 15 with row and plant spacings of 0·6 and 0·3 m, respectively. Based on standard cultivation techniques for maize in the region, 36 kg N ha^{-1} (urea), 120 kg P_2O_5 ha^{-1} (superphosphate) and 100 kg K_2O ha^{-1} (potassium sulfate) were applied before sowing as a base fertilizer, and 84 kg N ha^{-1} (urea) was applied 52 days after sowing (DAS) as a top dressing. Weeds were removed by hand to avoid herbicide influences on crop growth.

Root-core sampling system

A custom-made system was used to sample the root systems of individual plants in the field. This comprised a demountable hammer module (Fig. 1), a sampling cylinder (Fig. 2A) and a demountable lift module (Fig. 2B). The sampling cylinder (50 cm diameter, 55 cm high) was made up of two half-cylinders each with cutting teeth on the lower edge. The two pieces were united by six fittings welded to the abutting edges (Fig. 2A). The screws on the top and bottom fittings only were inserted. A cross-bearing was attached to the top of the cylinder (Fig. 1; Supplementary Data Fig. S1A).

When the hammer module was operating, an electric motor (1·5 kW) with reduction gearing (reduction ratio = 1:40) set in motion a spindle mounted on top of a supporting pillar via a chain on the right-hand side of the module; this drove the chain in the middle of the supporting pillar. Two horizontal rods mounted on the chain in the middle of the supporting pillar engaged alternately with a spigot welded to the hammer and so lifted the hammer (approx. 50 kg). When the hammer had been lifted to the top of the supporting pillar, the rod disengaged from the spigot. This allowed the hammer, guided by a slideway, to fall so as to impact the cross-bearing which gradually drove the sampling cylinder into the soil (approx. 2 cm per impact).

When the sampling cylinder had been driven to the desired depth (approx. 50 cm) (Supplementary Data Fig. S1B), the cylinder with the root core (approx. 150 kg) was withdrawn using a demountable lift module (Fig. 2B; Supplementary Data Fig. S1C). A pulley (1·5 T) linked to a chain block (1·5 T) hung from the portal frame. Four steel ropes were attached to the chain block

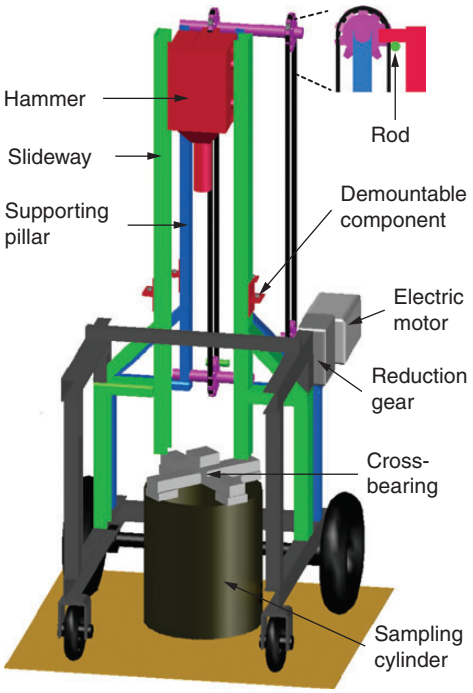

FIG. 1. Schematic of the hammer module of the custom-made root-core sampling system. The hammer module (1·1 m wide, 1·2 m deep, 2·2 m high) was used to force the sampling cylinder into the soil. A reduction gear driven by an electric motor drove the chain (top right of the diagram). Two rods mounted in symmetrical positions on the lifting chain (centre upper part of the module) lift the hammer alternately. A spigot welded to the hammer (top rear) engages with a rod to lift the hammer (detail top right of the diagram). The cross-bearing is placed on the sampling cylinder. The slideway and supporting pillars are demountable to allow the height of the hammer module to be adjusted.

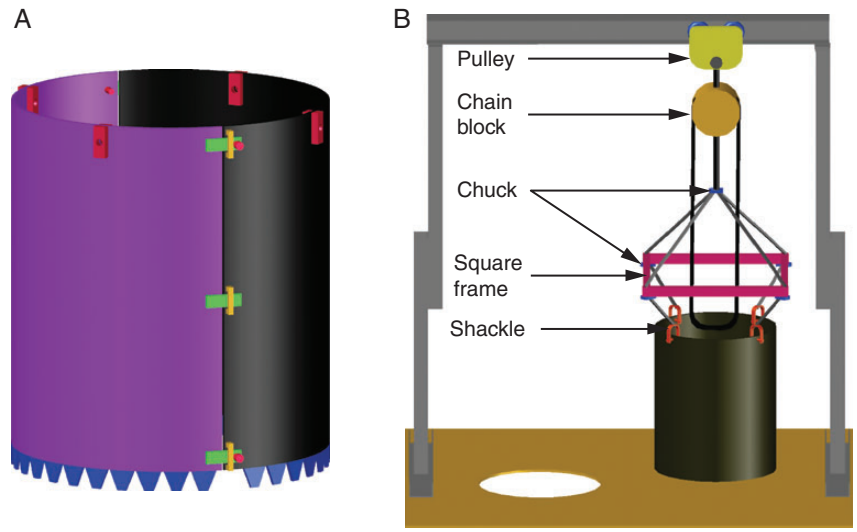

FIG. 2. Schematic of the sampling cylinder (A) and a demountable lift module (B) of the custom-made root-core sampling system. (A) The sampling cylinder (50 cm diameter, 55 cm high, 4 mm wall thickness) is composed of two half-cylinders with cutting teeth along the bottom edges. The two pieces are united by flanges welded along the abutting edges. Near the top edge of the sampling cylinder, four equidistant holes allow mounting of four U-shackles. (B) The lift module (1·5 m wide, 2 m high) was used to lift the sampling cylinder with a pulley and chain block. Four steel ropes are attached to the chain block at the top using steel rope chucks, which then pass through holes in the corners of a square frame, and at their lower ends they are fastened to the U-shackles using steel rope chucks.

by steel rope chucks. The steel ropes then passed through holes at the four corners of the square support frame and were fastened by steel rope chucks to four U-shackles mounted on the top edge of the sampling cylinder. The cylinder was lifted using the chain block. Because the length of the diagonal of the square frame was greater than the diameter of the sampling cylinder, the ropes had the additional function of pulling the top edges of the two half-cylinders slightly apart, so resulting in a slight compression at the lower end of the soil core which reduced its tendency to drop out during lifting (Supplementary Data Fig. S1C, D).

Root sampling and washing

At 19 d after silking (77 DAS), a maize plant was selected which represented the mean growth status of those in the plot. Its shoot was cut off before root sampling. The sampling cylinder was then placed on the soil surface over the plant stump and aligned with its axis. The root core was excavated using the sampling system. The total time required for set-up, driving the cylinder into the soil (3 min) and lifting the cylinder out of the soil (2·5 min) was approx. 20 min. The two half-cylinders were removed from the sample by releasing their edge fittings and separating the two halves (Supplementary Data Fig. S2A). The soil monolith was then eroded using a group of adjustable water jets (Supplementary Data Fig. S2B). To minimize root breakage during washing, a steel disc was fastened around the base of the root core (Supplementary Data Fig. S2B), and the angle and pressure of the jets were optimized. About 3 h was required for washing out a root system sample. The root system was then stored in a cool room at 3 °C.

Root separation and scanning

Each nodal root cut from the sampled root system was stored in a plastic box (Supplementary Data Fig. S3). Only nodal roots from the fourth to the seventh nodal root whorls were comparatively intact and suitable for further measurement. Seminal roots and nodal roots from the first to the third whorls were significantly decayed. Nodal roots from each of the whorls were grouped according to their visual similarity (i.e. the diameter and length of the axile root, the length of the unbranched zone, and the numbers and lengths of the first-order lateral roots) (Supplementary Data Fig. S3A–C). The number of nodal roots selected for root scanning depended on the number of groups in each whorl.

The unbranched zone of each axile root was scanned directly. The branching zone of the axile root of each of the selected nodal roots was cut into 5 cm sections from the base of the branching zone. Different scanning strategies were adopted depending on the complexity of the axile branching sections. These were classified according to the numbers and lengths of their lateral roots. Thus, for sections of low complexity, the axile branching section was scanned directly including its lateral roots (Supplementary Data Fig. S4A). For sections of medium complexity, the first-order lateral roots were cut from the axile root and then scanned together (Supplementary Data Fig. S4B). For sections of high complexity, the first-order lateral roots were first cut from the axile root and these were each cut into a number of parts (Supplementary Data Fig. S4C). To minimize root overlap in the scanning dishes, lateral roots were spread out by hand before scanning. Approximately 3 h was required to scan a nodal root. All roots were scanned at a resolution of 400 dpi.

Image processing

WinRHIZO Pro 2009b (Regent, Canada) was used to analyse the scanned root images. The noise in the original images was removed using the erasing tool, and pale roots, not recognized by the software, were emphasized using the filling tool. Incorrect topological connections were also identified and

rectified. The developmental (centrifugal) segment ordering system (Berntson, 1997) was used to record root topology.

Data processing

A lateral root unit (LRU) – a first-order lateral root with higher order laterals – was used to group data interpreted from the root images. The basic unit for measurement using WinRHIZO software is a 'link', being defined as a linear (unbranched) portion of a root section bounded at each end either by another root section or by a root tip. Contiguous groups of links of the same order are treated as a segment (Berntson, 1997). The software organizes the geometry (length) and topological connection (branching order, segment sequence, link sequence on the current segment and its mother segment sequence) of individual links.

Corresponding to the three different root scanning strategies, there were three different strategies for analysing the images using WinRHIZO. For an axile section with low complexity, the entire axile root section was selected and marked (Supplementary Data Fig. S5A). For an axile section of medium complexity, each first-order root was selected and marked with sequential numbers (Supplementary Data Fig. S5B). For an axile section of high complexity, the successive parts of each cut first-order lateral were marked with sequential numbers (Supplementary Data Fig. S5C). After analysis of a scanned image, the data were output to a .txt file by WinRHIZO software.

A program based on a Visual Basic Application (VBA) language embedded in Microsoft Excel™ was developed to batch the files to obtain the topological connections and geometrical data of individual LRUs. As any LRU of high complexity had been cut into pieces for scanning, these were sequentially merged to reconstitute the complete LRU. For axile branching sections of low complexity, each LRU was detached from the axile root by the program. Finally, the program exported a .csv file for individual nodal roots. Each row of the file contained the data for each link, e.g. the 5 cm section sequence, an LRU identifier, order, segment sequence, link sequence in the current segment, mother segment sequence (if applicable), link sequence on the mother segment (if applicable) and length. A package including the VBA program, a manual for using the VBA program and a file containing example data can be obtained by Emailing the author at wujie.cau@gmail.com. The length and diameter of the unbranched zone of the axile root and the diameter of each 5 cm axile root were measured using WinRHIZO software directly.

Visualization of the measured individual nodal roots

viRoot software was developed to reconstruct and visualize the measured individual nodal roots two-dimensionally (2-D) based on the extracted topological and geometrical data, so as to compare the scanned roots visually with the reconstructed roots. The software was built using C++ language, Boost libraries (www.boost.org), the SQLite relational database (www.sqlite.org) and the Visualisation Toolkit (www.vtk.org). Visualization was executed using ParaView software (www.paraview.org). The parameters used in viRoot software are given in Supplementary Data Fig. S6.

Root architectural trait derivations

Each nodal root was named using the whorl sequence ('N' plus its whorl sequence number) plus its rank of nodal root length in its whorl; for example, N6-2 indicates the nodal root with the second longest total root length in the sixth whorl. The RSA traits including the total number and length of laterals of different orders and LRUs of different ranks, and the distribution of these along the axile root of individual nodal roots, were computed. Data analysis was done using R software (R Development Core Team, 2013).

RESULTS

Two-dimensional architecture of individual lateral root units and individual nodal roots

Each sampled nodal root was cut into 5 cm axile root sections to avoid overlap in scanning. Some LRUs of the axile root sections were cut and scanned solely because of their high complexity. Figure 3A shows an LRU which had the highest complexity and total length among LRUs in all the sampled nodal roots of the measured maize plant. This LRU was further cut into portions for scanning (Fig. 3B). A few selected second-order laterals in the scanned image were marked with numbers for visual comparison with the corresponding laterals in the LRU reconstructed using viRoot software (Fig. 3C). The number and length of laterals and their topological connections of these marked laterals of the scanned and reconstructed LRU were visually close. To assess further the reliability of our VBA program in organizing the data output from WinRHIZO software, two scanned and reconstructed LRUs were compared (Supplementary Data Table S1). Figure 4 shows the measured individual nodal roots from different whorls of the maize plant. The variations were significant in number and length of laterals of different orders along axile roots and among individual nodal roots.

Lateral order, number and length of individual nodal roots

The first 30 cm branching zone of each axile root was used in the following comparisons of architectural traits among nodal roots, since axile roots did not have equal length and the minimum length of the axile branching zone of the sampled nodal roots was 30 cm (Fig. 4). The highest branching order was five for N5-2, N6-1, N6-4 and N7-1. Other nodal roots had four-order branching, except N4-2 in which only three-order branching was observed.

The total length and number of lateral roots of individual nodal roots varied substantially (Fig. 5). The largest length and number of lateral roots occurred in N6-1. The total root length was mainly contributed by first- and second-order laterals for individual nodal roots (Fig. 5A). Second-order laterals made up the largest portion of the total lateral number, ranging from 48 to 79 % for all sampled nodal roots except nodal root N4-2 (Fig. 5B). First-order laterals constituted a large fraction of the total lateral root length, while they did not make up a large portion of the total number (Fig. 5). For some nodal roots, third-order laterals accounted for a substantial part of the total number and length, especially for N6-1 and N7-1. The number of fourth-order laterals was small but significant for N6-1 and N7-1 (approx. 3 % of the total number of laterals for these nodal roots), while their lengths were negligible

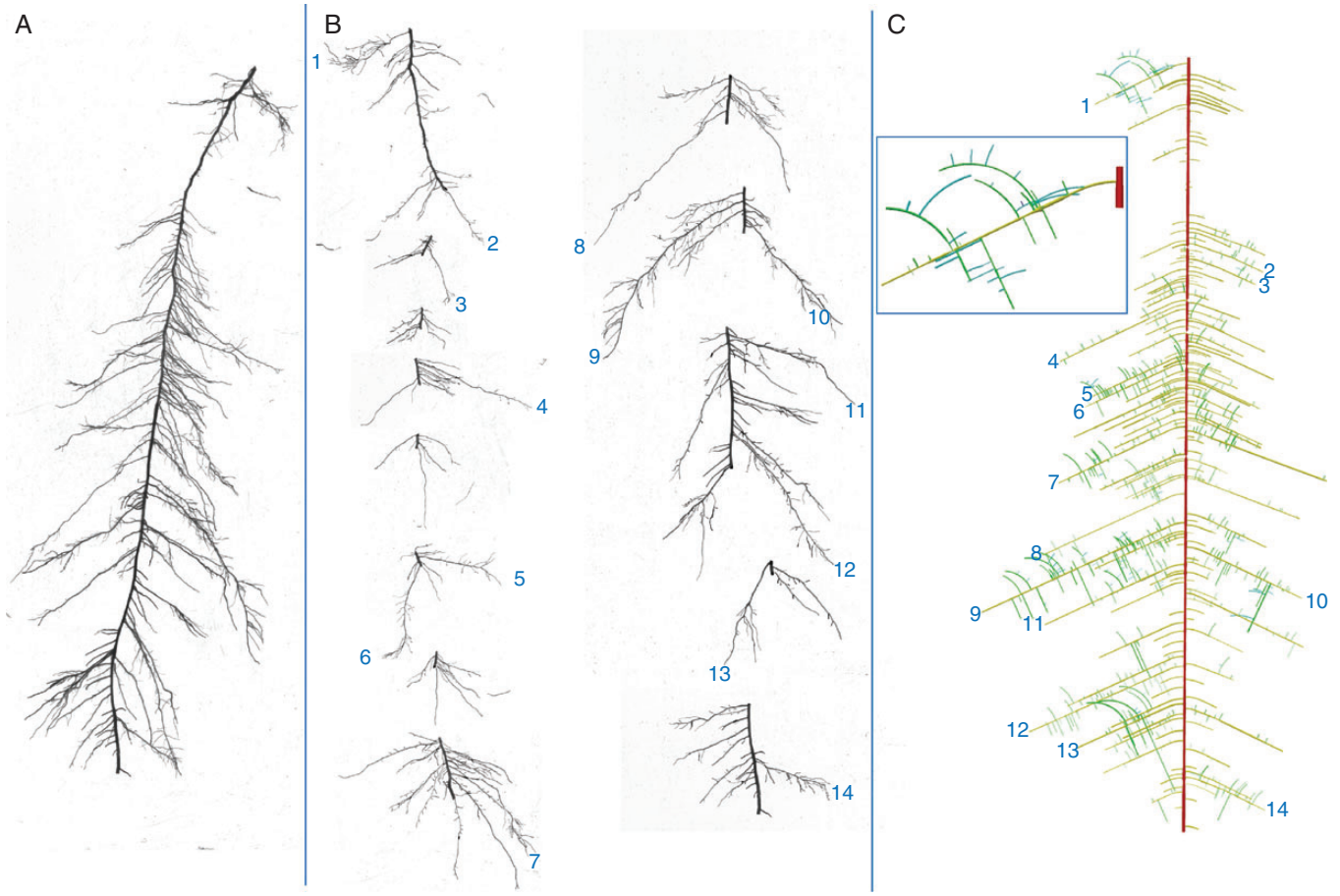

FIG. 3. The scanning and analysis of a lateral root unit (LRU, i.e. a first-order lateral root with higher order laterals) with high architectural complexity. (A) The scanned LRU; (B) the scanned image of the cut LRU sections. The cut sections of the LRU were arranged sequentially and spread before scanning to avoid overlap. (C) 2-D architecture of the LRU reconstructed using viRoot software. Different colours indicate laterals of different orders. Numbers were marked for comparison of lateral distribution in the scanned LRU with that in the reconstructed LRU. This LRU was cut from the first 5 cm axile branching section of the longest nodal root in the sixth whorl of a maize plant. The length of the first-order lateral of this LRU was 24·3 cm. The inset in C shows the magnification of the first group of laterals.

(Fig. 5A). Both the number and length of the fifth-order laterals were negligible.

Distribution in individual root lengths of laterals of different orders

Since high-order (i.e. fourth- and fifth-order) lateral roots occurred only on some nodal roots, we compared the individual root lengths of first-, second- and third-order lateral roots among the nodal roots. The average individual root length of laterals of a specific order was always significantly larger than their median values for individual nodal roots (Fig. 6). The median and average individual root lengths of lower order laterals were larger than those of higher order laterals for each nodal root. Median and average individual root lengths of the first-order laterals were significantly larger (by at least three times) than those of the second-order laterals.

Median and average values of the first-order laterals were in the range 0·5–2·5 cm and 1–4 cm, respectively. The highest average values of the second- and third-order laterals were >0·6 cm and 0·3 cm, respectively. In contrast, the maximum individual root length of the first-order laterals was 30·3 cm (recorded in N6-2), that of second-order laterals was 9·4 cm (recorded in N5-1) and that of third-order laterals was 3·2 cm (recorded in N7-1).

The root length distribution of laterals of different orders was highly asymmetrical, and the log-normal curve fitted the distribution well for nodal roots from individual whorls (Fig. 7). The mode of the distribution was 0·5–1 cm for first-order laterals, 0–0·2 cm for second-order laterals and 0–0·1 cm or 0·1–0·2 cm for third-order laterals. Nevertheless, the probability density of the modes for distinct whorls varied and no systematic trend was observed among whorls.

Length and number of lateral root units of individual nodal roots

As an LRU refers to a first-order lateral with higher order lateral roots derived from it, the rank of an LRU was defined according to its highest branching order. The number of the first-rank LRUs (i.e. first-order laterals without higher order laterals arising from them) comprised at least 54 % of the total LRU number for all nodal roots, and up to 80 % for that of N4-2 (Fig. 8A). The total number of the second-rank LRUs comprised in the range 17–35 % of the total LRU number. Third- and higher rank LRUs accounted for a small portion of the total LRU number. For a given nodal root, the higher its LRU rank, the smaller its LRU number.

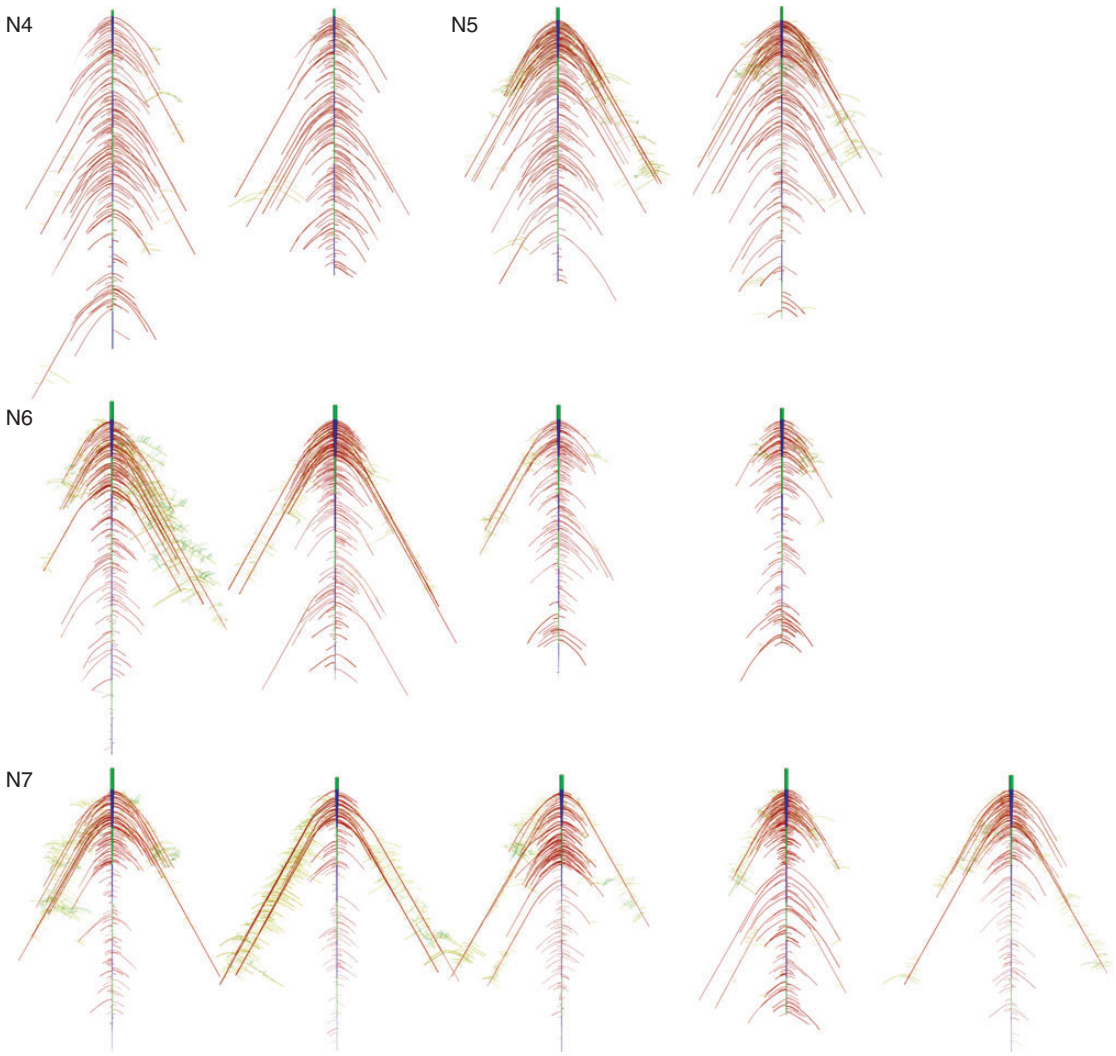

FIG. 4. Visualization of the 2-D architecture of individual nodal roots from different whorls of a maize plant. For an axile root, the first green section indicates the unbranched zone and the following blue and green sections alternately indicate different 5 cm sections. For lateral roots, different colours indicate laterals of different orders. The number following 'N' indicates the whorl sequence of the given nodal roots.

Although the first- and second-rank LRUs constituted a large percentage of the total LRU number, their contribution to the total LRU length was small (Fig. 8B). In contrast, a small number of LRUs with high rank contributed a large part of the total length of LRUs for individual nodal roots. For example, the third- and higher rank LRUs made up <15 % of the total number of LRUs in N7-1, N7-2 and N7-6 (Fig. 8A). In contrast, they contributed >70 % of the total LRU length (Fig. 8B). In an extreme case, two fifth-rank LRUs contributed >20 % of total lateral root length in N6-1 (Fig. 8).

Laterals in the first 5 cm axile branching section

For a given nodal root, the highest order laterals always occurred in the first 5 cm axile branching section, and, for most nodal roots, only this section had the highest order laterals. Laterals in the first 5 cm axile branching section contributed dominantly to total length and number of laterals for each nodal root, with the exception of the oldest nodal roots (N4-1 and N4-2) (Fig. 9). Laterals in the first 5 cm axile branching section (one-sixth the length of the axile branching zone) made up 54–89 % and 60–92 %, respectively, of the total lateral length and number of laterals of different order of a nodal root (Fig. 9).

DISCUSSION

We present here an integrated method for root sampling, root architecture analysis and reconstruction of individual field-grown crop plants such as maize. The major part of an individual root system can first be excavated with the component roots still relatively intact. A combination of a proprietary software and a novel program was used for collecting individual RSA information. Software (viRoot) was developed to reconstruct and visualize individual nodal roots based on extracted geometrical and topological data. The technique is introduced by applying it to the study of the root system of a field-grown maize plant at a

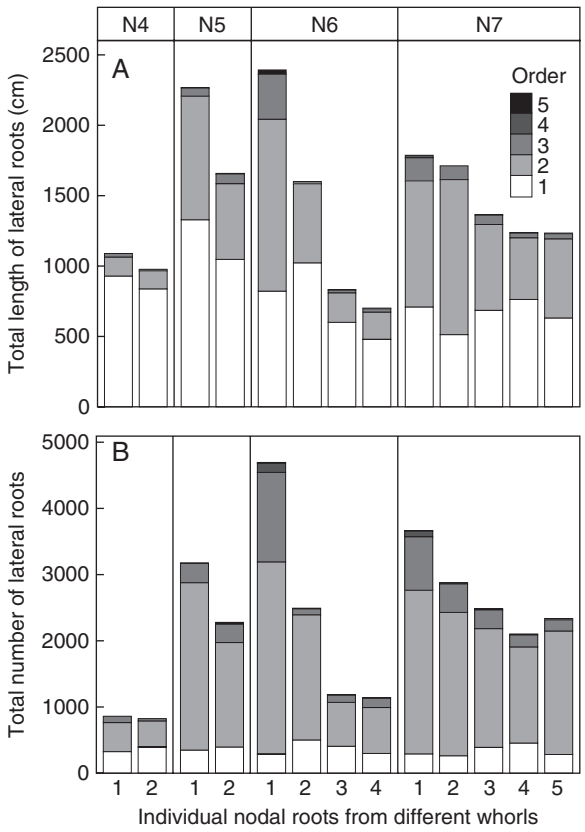

FIG. 5. Total root length (A) and number (B) of laterals of different orders for individual nodal roots of a maize plant. The number following 'N' indicates the whorl sequence of the given nodal roots.

stage 19 d after silking and by presenting a 2-D visualization of individual nodal roots and an analysis of the results.

The significance for quantification of high-order root branching

In recent years, researchers have paid increasing attention to questions of root branching. A proposal for a set of minimum criteria for meaningful RSA measurement (root length, root mass and root number) has been made for realizing the power of comparative genetics (de Dorlodot *et al.*, 2007). Quantifying the topological and geometrical architecture of root systems of mature field-grown crops should provide new information for genetics research. However, in the literature, only the architectural traits of lower order laterals have been measured for crop plants. Commonly, the number and length distribution of first-order laterals along an axile root have been quantified (Varney *et al.*, 1991; Pagès and Pellerin, 1994; Enns *et al.*, 2006; Ito *et al.*, 2006), while only the branching density of second-order laterals on the first-order laterals has been analysed (Pagès and Pellerin, 1994).

Clearly, maize has the potential for much higher order root branching than this. Thus, Yamauchi *et al.* (1987) observed fourth-order lateral roots in the root systems of box-grown maize plants, and we detected fifth-order lateral roots in our root systems (Fig. 5). It should also be noted that lateral roots having higher order branches represent a significant proportion of the whole, in terms both of root number and of total root length. For example, up to 65 % of the total length of lateral roots is contributed by second- or higher order branches in N6-1 (Fig. 5A). The considerable length of the high-order laterals may reflect a plasticity in root growth and a feedback response to heterogeneity in soil nutrients and other resources in

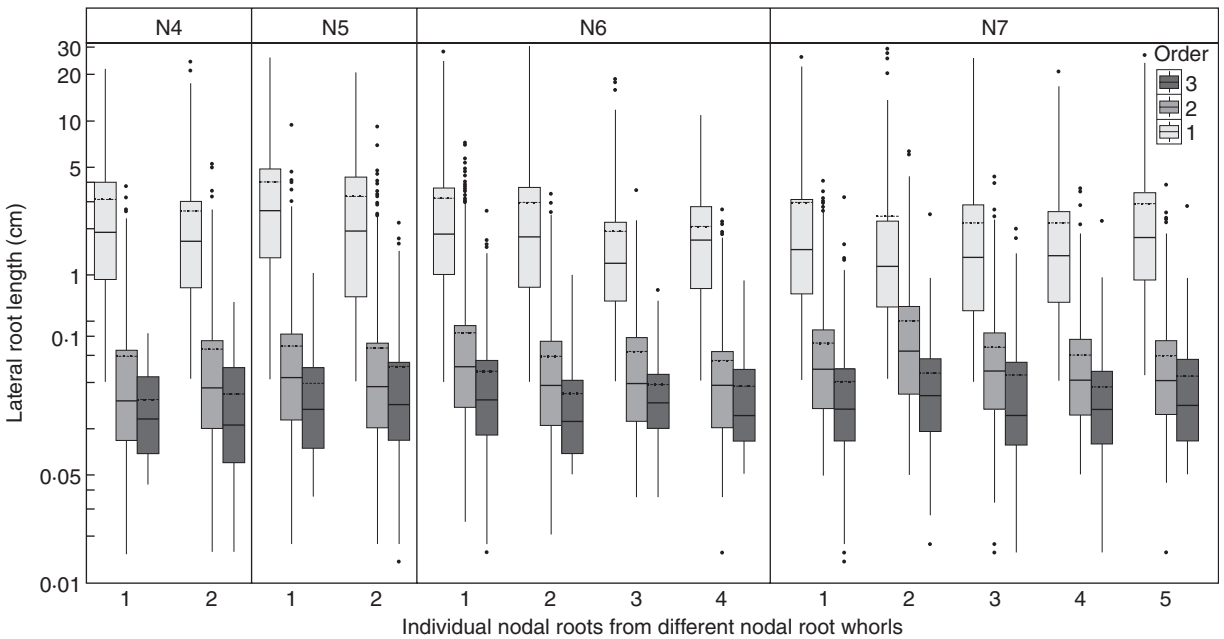

FIG. 6. Length variation of lateral roots of different orders for individual nodal roots of a maize plant. Horizontal line, median; box, median ± 25 %; dashed line, average; black dots, statistical outliers lower and higher than 5 and 95 % quantiles, respectively. The *y*-axis scale is logarithmically transformed. The number following 'N' indicates the whorl sequence of the given nodal roots.

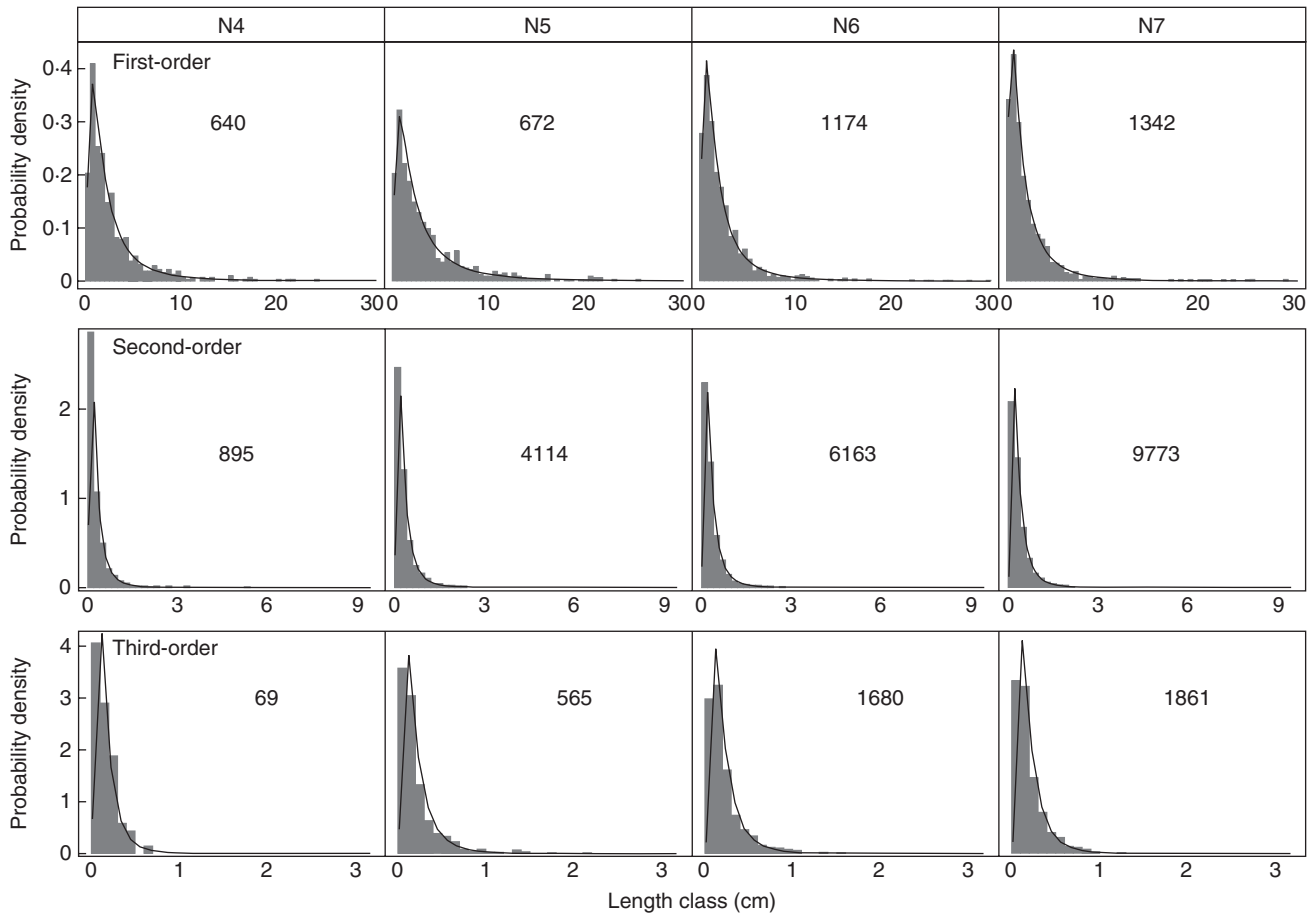

FIG. 7. Probability density histogram of root lengths of laterals of different orders for nodal roots from the same whorl of a maize plant. The length classes for the first-, second- and third-order laterals were 0·5, 0·2 and 0·1 cm, respectively. The curve indicates the fitted log-normal distribution. The number in each panel indicates the number of laterals used. The number following 'N' indicates the whorl sequence of the given nodal roots.

the rhizosphere (Hodge, 2004). Thus increases in the total length and surface area of a root system will enable a plant to tap more distant reserves of soil water and nutrients (Smith and Smet, 2012). In addition, second- and higher order laterals represent >60 % of the lateral root number of the root systems of box-grown maize plants (Iijima *et al.*, 1991). In our measurement, the number of second- and higher order laterals represented even larger proportions of the total lateral root numbers (e.g. 93 % for N6-1) (Fig. 5B). High numbers of lateral roots imply large numbers of root tips, which are associated with many vital aspects of root function (Forde, 2009).

In our study, root length of the same order laterals of field-grown maize was highly variable, and short roots contributed a substantial fraction to the total length. These small lateral roots in maize are probably short lived and/or determinate in growth pattern (Cahn *et al.*, 1989; Varney *et al.*, 1991), or have a vascular system so reduced as to be almost totally ineffective in water and nutrient delivery since high axial resistance exists in the first 2 cm from the root apex due to the differentiation of the early metaxylem vessel (Frensch and Steudle, 1989). To understand the discrepancy in potential functionality of laterals with different types, orders and lengths growing under field conditions, their difference in anatomical structure should be investigated in a further study.

Branching capacity of individual LRUs and the proximal axile branching zone

In this study, the branching characteristics of individual LRUs for individual nodal roots were analysed. Although the total number and length of up to fourth-order laterals collected from different types of roots were calculated (Yamauchi *et al.*, 1987; Iijima *et al.*, 1991), these studies did not determine the topological relationships of these laterals of different orders to individual LRUs for each root type. For all nodal roots in our study, the higher the LRU rank, the lower their number (Fig. 8A). Although high-rank LRUs occupied only a small proportion of the total number of LRUs, they contributed a large part of the total length of LRUs for individual nodal roots (Fig. 8B). In an extreme case, >20 % of total lateral root length in N6-1 was contributed by two fifth-rank LRUs (Fig. 8).

Abundant branching capacity was observed in the first 5 cm axile branching section in our study. For most nodal roots, laterals in this root section occupied more than half of the total length and number of each nodal root (Fig. 9). The highest order laterals occurred only in this section for most nodal roots. Therefore, quantification of branching capacity and characteristics of LRUs and the proximal axile branching zone may provide valuable new information on root systems.

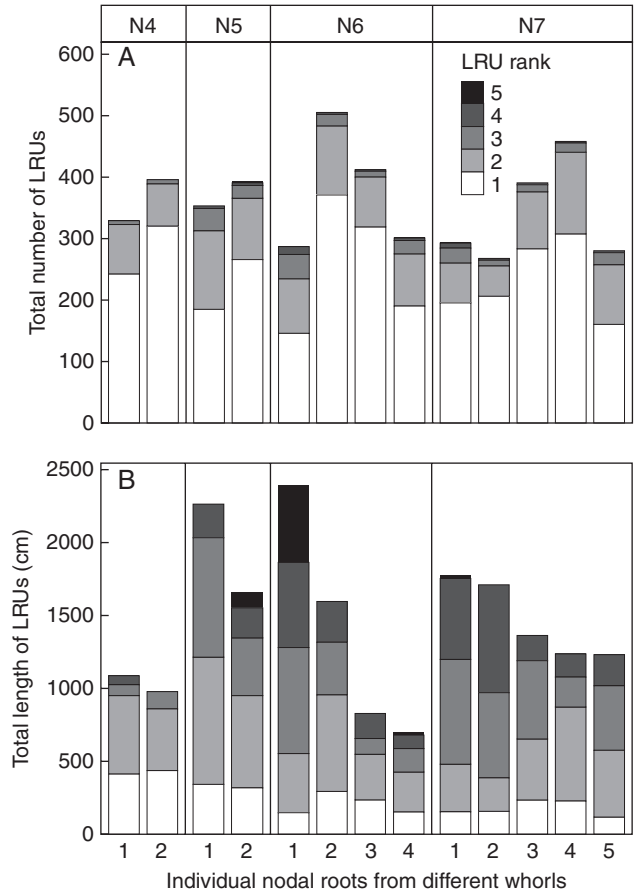

FIG. 8. Total number (A) and length (B) of lateral root units (LRUs), individual first-order lateral roots with the higher order laterals derived from them, for individual nodal roots of a maize plant. The rank of an LRU was determined according to its highest branching order, and the length of an LRU was determined by adding together the length of its laterals of different orders. The number following 'N' indicates the whorl sequence of the given nodal roots.

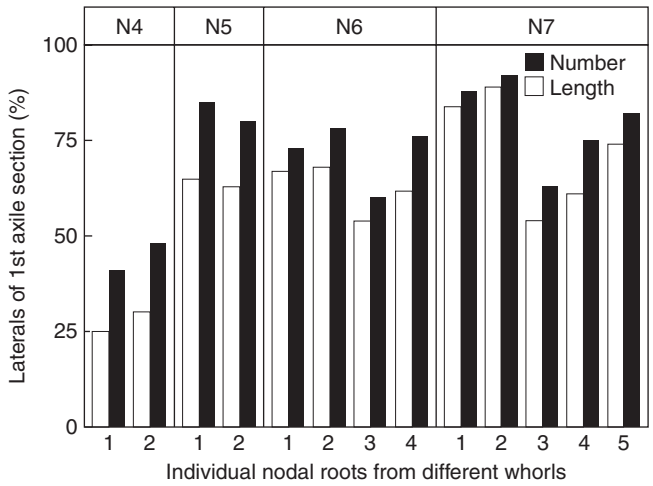

FIG. 9. The percentage of the number and total length of laterals of different orders of the first 5 cm axile root sections of individual nodal roots. The number following 'N' indicates the whorl sequence of the given nodal roots.

Potential applications and improvement of the root-core sampling method

The spatial distribution of root length density (RLD) has a large impact on water and nutrient uptake of individual plants (Waisel *et al.*, 2002). The root auger method has been applied extensively for estimating RLD (Bohm, 1979; Oliveira *et al.*, 2000). However, auger diameter, sampling positions, number of replications and even the weighting factor for cores sampled from different positions affect the reliability of RLD estimation using the auger method (Mengel and Barber, 1974; van Noordwijk *et al.*, 1985; Kumar *et al.*, 1993; Gajri *et al.*, 1994; Buczko *et al.*, 2009). As most of the root length or mass of maize at silking is located in the topsoil (Mengel and Barber, 1974; Dwyer *et al.*, 1996; Oikeh *et al.*, 1999; Kuchenbuch *et al.*, 2009), our system can be regarded as a large, though short, root auger (50 cm diameter) for analysing whole RLD directly, and thus provides reliable data for evaluating different schemes of root auger sampling. However, this method may not be suitable for quantifying deep roots, which is particularly important for drought environments and for recapturing leached nutrients. Concerning the excavation of different size framed monoliths, our system, which could excavate a medium monolith (Supplementary Data Table S2), can be considered as requiring low time and manpower consumption, low cost of machinery, no extra soil disturbance while lifting out the corer, and less soil compaction because of its relatively low weight and optimizable tyre width. Furthermore, the size and shape of the sampling cylinder could be modified for specific objectives.

Perspectives

Considerable attention has been paid to the potential to accelerate crop improvement by introducing both intrinsic and environmentally responsive root architectural characteristics into breeding programmes (de Dorlodot *et al.*, 2007; Lynch and Brown, 2012). High-throughput phenotyping of young root systems grown in gellan gum, hydroponic or semi-hydroponic systems, or root boxes with soil medium is becoming an efficient approach for identifying, evaluating and selecting ideal RSA traits or genotypes (Iyer-Pascuzzi *et al.*, 2010; Chen *et al.*, 2011; Clark *et al.*, 2011, 2013; Nagel *et al.*, 2012; Galkovskyi *et al.*, 2012). However, it is critically important to determine whether these genotypes, screened under controlled conditions, are able to perform similarly in the field. Therefore, establishing relationships between high-throughput screening of root phenotypes in the laboratory and field screening of RSA traits will be of critical importance.

To be practicable, the new excavation techniques must be low cost in terms of capital investment in equipment and also low cost in terms of their use, i.e. simple and quick and not manpower intensive. The integrated technique we proposed offers a promising solution for excavation. Because our technique is able to provide a relatively complete set of root architectural information, it could be of use as a benchmark for evaluating other less demanding, field sampling methods. It may also be used to generate valuable new data for the parameterization of other root architectural models (Dunbabin *et al.*, 2013).

SUPPLEMENTARY DATA

Supplementary data are available online at www.aob.oxfordjournals.org and consist of the following. Figure S1: images of maize root sampling in the field using the custom-made root-core sampling system. Fig. S2: images of the root core sample. Fig. S3: individual nodal roots sampled from the seventh nodal root whorl of a maize plant at 19 d after silking. Fig. S4: scanned root images. Fig. S5: analysis of root images using WinRHIZO Pro software. Fig. S6: parameters of viRoot software. Table S1: comparison of scanned and reconstructed LRUs using output from WinRHIZO Pro software based on scanning images. Table S2: comparison of field excavation methods of the root system.

ACKNOWLEDGEMENTS

This work was supported by the National Natural Science Foundation of China (41071205) and the National Scientific and Technological Support Plan (2012BAD35B02). We would like to thank Jie Zhou, Bo Yang and Qi Shen for their help in conducting experiments, image processing and data extraction, Zhili Gong for his technical help in designing and manufacturing of the hammering module and lift module, Qian Wu for her kind help with figure drawing, and Dr Loïc Pagès (INRA) and Professor Chunjian Li (CAU) for their valuable comments on the manuscript.

LITERATURE CITED

Armengaud P, Zambaux K, Hills A, *et al*. 2009. EZ-Rhizo: integrated software for the fast and accurate measurement of root system architecture. *The Plant Journal* **57**: 945–956.

Berntson GM. 1997. Topological scaling and plant root system architecture: developmental and functional hierarchies. *New Phytologist* **135**: 621–634.

Bohm W. 1979. *Methods of studying root systems.* Berlin: Springer-Verlag.

Bouma TJ, Nielsen KL, Van Hal J, Koutstaal B. 2001. Root system topology and diameter distribution of species from habitats differing in inundation frequency. *Functional Ecology* **15**: 360–369.

Brown DP, Pratum TK, Bledsoe C, Ford ED, Cothern JS, Perry D. 1991. Noninvasive studies of conifer roots: nuclear magnetic resonance (NMR) imaging of Douglas-fir seedlings. *Canadian Journal of Forest Research* **21**: 1559–1566.

Buczko U, Kuchenbuch RO, Gerke HH. 2009. Evaluation of a core sampling scheme to characterize root length density of maize. *Plant and Soil* **316**: 205–215.

Cahn M, Zobel R, Bouldin D. 1989. Relationship between root elongation rate and diameter and duration of growth of lateral roots of maize. *Plant and Soil* **119**: 271–279.

Chen YL, Dunbabin VM, Diggle AJ, Siddique KHM, Rengel Z. 2011. Development of a novel semi-hydroponic phenotyping system for studying root architecture. *Functional Plant Biology* **38**: 355–363.

Clark RT, MacCurdy RB, Jung JK, *et al*. 2011. Three-dimensional root phenotyping with a novel imaging and software platform. *Plant Physiology* **156**: 455–465.

Clark RT, Famoso AN, Zhao K, *et al*. 2012. High-throughput two-dimensional root system phenotyping platform facilitates genetic analysis of root growth and development. *Plant, Cell and Environment* **36**: 454–456.

Danjon F, Reubens B. 2008. Assessing and analyzing 3D architecture of woody root systems, a review of methods and applications in tree and soil stability, resource acquisition and allocation. *Plant and Soil* **303**: 1–34.

Dittmer HJ. 1937. A quantitative study of the roots and root hairs of a winter rye plant (Secale cereale). *American Journal of Botany* **24**: 417–420.

De Dorlodot S, Forster B, Pagčs L, Price A, Tuberosa R, Draye X. 2007. Root system architecture: opportunities and constraints for genetic improvement of crops. *Trends in Plant Science* **12**: 474–481.

Dubrovsky JG, Forde BG. 2012. Quantitative analysis of lateral root development: pitfalls and how to avoid them. *The Plant Cell* **24**: 4–14.

Dunbabin VM, Postma JA, Schnepf A, *et al*. 2013. Modelling root–soil interactions using three-dimensional models of root growth, architecture and function. *Plant and Soil* **372**: 93–124.

Dwyer LM, Ma BL, Stewart DW, *et al*. 1996. Root mass distribution under conventional and conservation tillage. *Canadian Journal of Soil Science* **76**: 23–28.

Enns LC, McCully ME, Canny MJ. 2006. Branch roots of young maize seedlings, their production, growth, and phloem supply from the primary root. *Functional Plant Biology* **33**: 391–399.

Fang S, Yan X, Liao H. 2009. 3D reconstruction and dynamic modeling of root architecture *in situ* and its application to crop phosphorus research. *The Plant Journal* **60**: 1096–1108.

Fiorani F, Schurr U. 2013. Future scenarios for plant phenotyping. *Annual Review of Plant Biology* **64**: 267–291.

Fitter AH. 1987. An architectural approach to the comparative ecology of plant root systems. *New Phytologist* **106**: 61–77.

Flavel RJ, Guppy CN, Tighe M, Watt M, McNeill A, Young IM. 2012. Non-destructive quantification of cereal roots in soil using high-resolution X-ray tomography. *Journal of Experimental Botany* **63**: 2503–2511.

Forde BG. 2009. Is it good noise? The role of developmental instability in the shaping of a root system. *Journal of Experimental Botany* **60**: 3989–4002.

Frensch J, Steudle E. 1989. Axial and radial hydraulic resistance to roots of maize (Zea mays L.). *Plant Physiology* **91**: 719.

Gajri PR, Arora VK, Kumar K. 1994. A procedure for determining average root length density in row crops by single-site augering. *Plant and Soil* **160**: 41–47.

Galkovskyi T, Mileyko Y, Bucksch A, *et al*. 2012. GiA Roots: software for the high throughput analysis of plant root system architecture. *BMC Plant Biology* **12**: 116.

Gregory PJ, Bengough AG, Grinev D, *et al*. 2009. Root phenomics of crops: opportunities and challenges. *Functional Plant Biology* **36**: 922–929.

Gruber BD, Giehl RFH, Friedel S, von Wirén N. 2013. Plasticity of the Arabidopsis root system under nutrient deficiencies. *Plant Physiology* **163**: 161–179.

Hackett C, Rose D. 1972. A model of the extension and branching of a seminal root of barley, and its use in studying relations between root dimensions I. The model. *Australian Journal of Biological Sciences* **25**: 669–680.

Hochholdinger F, Woll K, Sauer M, Dembinsky D. 2004. Genetic dissection of root formation in maize (Zea mays) reveals root-type specific developmental programmes. *Annals of Botany* **93**: 359–368.

Hodge A. 2004. The plastic plant: root responses to heterogeneous supplies of nutrients. *New Phytologist* **162**: 9–24.

Hodge A. 2006. Plastic plants and patchy soils. *Journal of Experimental Botany* **57**: 401–411.

Iijima M, Kono Y, Yamauchi A, Pardales JR Jr. 1991. Effects of soil compaction on the development of rice and maize root systems. *Environmental and Experimental Botany* **31**: 333–342.

Ito K, Tanakamaru K, Morita S, Abe J, Inanaga S. 2006. Lateral root development, including responses to soil drying, of maize (Zea mays) and wheat (Triticum aestivum) seminal roots. *Physiologia Plantarum* **127**: 260–267.

Iyer-Pascuzzi AS, Symonova O, Mileyko Y, *et al*. 2010. Imaging and analysis platform for automatic phenotyping and trait ranking of plant root systems. *Plant Physiology* **152**: 1148 –1157.

Jahnke S, Menzel MI, Van Dusschoten D, *et al*. 2009. Combined MRI–PET dissects dynamic changes in plant structures and functions. *The Plant Journal* **59**: 634–644.

Kuchenbuch RO, Gerke HH, Buczko U. 2009. Spatial distribution of maize roots by complete 3D soil monolith sampling. *Plant and Soil* **315**: 297–314.

Kumar K, Prihar SS, Gajri PR. 1993. Determination of root distribution of wheat by auger sampling. *Plant and Soil* **149**: 245–253.

Lynch J. 1995. Root architecture and plant productivity. *Plant Physiology* **109**: 7.

Lynch JP, Brown KM. 2012. New roots for agriculture: exploiting the root phenome. *Philosophical Transactions of the Royal Society B: Biological Sciences* **367**: 1598–1604.

Mairhofer S, Zappala S, Tracy SR, *et al*. 2012. RooTrak: automated recovery of three-dimensional plant root architecture in soil from x-ray microcomputed tomography images using visual tracking. *Plant Physiology* **158**: 561 –569.

Malamy JE. 2005. Intrinsic and environmental response pathways that regulate root system architecture. *Plant, Cell and Environment* **28**: 67–77.

McCully ME. 1999. Roots in soil: unearthing the complexities of roots and their rhizospheres. *Annual Review of Plant Biology* **50**: 695–718.

Mengel DB, Barber SA. 1974. Development and distribution of the corn root system under field conditions. *Agronomy Journal* **66**: 341–344.

Menzel MI, Oros-Peusquens A-M, Pohlmeier A, Shah NJ, Schurr U, Schneider HU. 2007. Comparing 1H-NMR imaging and relaxation mapping of German white asparagus from five different cultivation sites. *Journal of Plant Nutrition and Soil Science* **170**: 24–38.

Mooney S, Pridmore T, Helliwell J, Bennett M. 2012. Developing X-ray computed tomography to non-invasively image 3-D root systems architecture in soil. *Plant and Soil* **352**: 1–22.

Moradi AB, Carminati A, Vetterlein D, *et al*. 2011. Three-dimensional visualization and quantification of water content in the rhizosphere. *New Phytologist* **192**: 653–663.

Nagel KA, Putz A, Gilmer F, *et al*. 2012. GROWSCREEN-Rhizo is a novel phenotyping robot enabling simultaneous measurements of root and shoot growth for plants grown in soil-filled rhizotrons. *Functional Plant Biology* **39**: 891–904.

Nelson WW, Allmaras RR. 1969. An improved monolith method for excavating and describing roots. *Agronomy Journal* **61**: 751–754.

Nibau C, Gibbs DJ, Coates JC. 2008. Branching out in new directions: the control of root architecture by lateral root formation. *New Phytologist* **179**: 595–614.

van Noordwijk M, Floris J, de Jager A. 1985. Sampling schemes for estimating root density distribution in cropped fields. *Netherlands Journal of Agricultural Science* **33**: 241–261.

Oikeh S, Kling J, Horst W, Chude V, Carsky R. 1999. Growth and distribution of maize roots under nitrogen fertilization in plinthite soil. *Field Crops Research* **62**: 1–13.

Oliveira MRG, van Noordwijk M, Gaze SR, *et al*. 2000. Auger sampling, ingrowth cores and pinboard methods. In: Smit DAL, Bengough DAG, Engels PDC, van Noordwijk DM, Pellerin DS, van de Geijn DSC, eds. *Root methods*. Springer: Berlin, 175–210.

Pagès L, Pellerin S. 1994. Evaluation of parameters describing the root system architecture of field grown maize plants II. Density, length, and branching of first-order lateral roots. *Plant and Soil* **164**: 169–176.

Pavlychenko TK. 1937. Quatitative study of the entire root systems of weed and crop plants under field conditions. *Ecology* **18**: 62–79.

Peng Y, Niu J, Peng Z, Zhang F, Li C. 2010. Shoot growth potential drives N uptake in maize plants and correlates with root growth in the soil. *Field Crops Research* **115**: 85–93.

Pohlmeier A, Oros-Peusquens A, Javaux M, *et al*. 2008. Changes in soil water content resulting from Ricinus root uptake monitored by magnetic resonance imaging. *Vadose Zone Journal* **7**: 1010–1017.

Poorter H, Bühler J, van Dusschoten D, Climent J, Postma JA. 2012. Pot size matters: a meta-analysis of the effects of rooting volume on plant growth. *Functional Plant Biology* **39**: 839–850.

Rascher U, Blossfeld S, Fiorani F, *et al*. 2011. Non-invasive approaches for phenotyping of enhanced performance traits in bean. *Functional Plant Biology* **38**: 968–983.

R Development Core Team. 2013. *R: a language and environment for statistical computing*. R Foundation for Statistical Computing, Vienna, Austria. http://www.R-project.org/.

Rogers HH, Bottomley PA. 1987. *In situ* nuclear magnetic resonance imaging of roots: influence of soil type, ferromagnetic particle content, and soil water. *Agronomy Journal* **79**: 957–965.

Smith S, Smet ID. 2012. Root system architecture: insights from Arabidopsis and cereal crops. *Philosophical Transactions of the Royal Society B: Biological Sciences* **367**: 1441–1452.

Trachsel S, Kaeppler SM, Brown KM, Lynch JP. 2010. Shovelomics: high throughput phenotyping of maize (Zea mays L.) root architecture in the field. *Plant and Soil* **341**: 75–87.

Varney G, Canny M, Wang X, McCully M. 1991. The branch roots of Zea. I. First order branches, their number, sizes and division into classes. *Annals of Botany* **67**: 357.

Waisel Y, Eshel A, Kafkafi U. 2002. *Plant roots: the hidden half*. Boca Raton, FL: CRC Press.

Weaver JE, Kramer J, Reed M. 1924. Development of root and shoot of winter wheat under field environment. *Ecology* **5**: 26.

Yamauchi A, Kono Y, Tatsumi J. 1987. Quantitative analysis on root system structures of upland rice and maize. *Japanese Journal of Crop Science* **56**: 608–617.